

See discussions, stats, and author profiles for this publication at: <https://www.researchgate.net/publication/239523340>

Dynamics of Cyclic Methylphenyltrisiloxane in the Picosecond to Nanosecond Time Range

DATASET · AUGUST 1999

CITATIONS

8

READS

11

5 AUTHORS, INCLUDING:



Fernando Dias

Durham University

66 PUBLICATIONS 1,436 CITATIONS

SEE PROFILE



João Carlos Lima

New University of Lisbon

143 PUBLICATIONS 2,213 CITATIONS

SEE PROFILE



Antonio Macanita

Technical University of Lisbon

126 PUBLICATIONS 2,424 CITATIONS

SEE PROFILE

ARTICLES

Dynamics of Cyclic Methylphenyltrisiloxane in the Picosecond to Nanosecond Time Range

Fernando B. Dias,[†] João C. Lima,[†] Antonio L. Maçanita,^{†,‡} Arturo Horta,^{*,§} and Inés F. Piérola[§]

Instituto de Tecnologia Química e Biológica (ITQB), Oeiras, Portugal, Instituto Superior Técnico (IST), UTL, Lisboa, Portugal, and Departamento de Fisicoquímica (CTFQ), Universidad a Distancia (UNED), Madrid, Spain

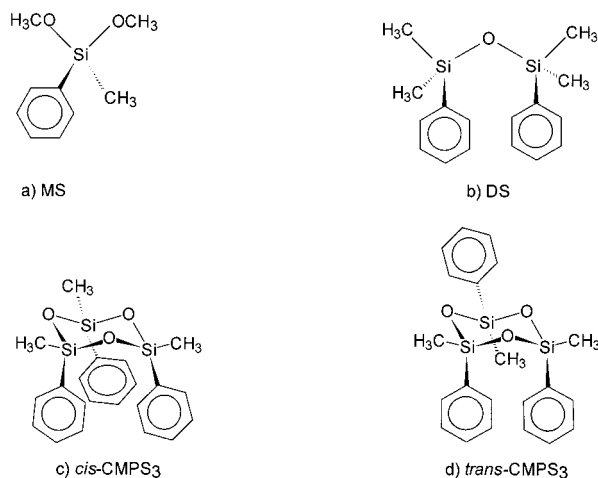
Received: August 25, 1999; In Final Form: October 21, 1999

The dynamics of the cyclic trimer of methylphenyl-substituted siloxane (1,3,5-triphenyl-1,3,5-trimethylcyclotrisiloxane; CMPS3) in dilute methylcyclohexane solution was probed with picosecond time-resolved and steady-state fluorescence in a wide range of temperatures (20 to $-100\text{ }^{\circ}\text{C}$) from the high-temperature limit to the low-temperature limit. The crossover between these two regimes is found around $-30\text{ }^{\circ}\text{C}$. Monomer and excimer decays are triexponential, with one of the three components coming from the monomer that is unable to form excimer with its neighboring chromophores (the lone phenyl ring in the trans isomer of CMPS3). A kinetic mechanism is developed that takes into account preformed dimers, lone monomers, and also energy transfer from these lone monomers to excimer-forming ones. With such a mechanism, the rate constants for excimer formation (k_a) and excimer dissociation (k_d), as well as the corresponding activation energies (E_a , E_d), are obtained from the decays. The rate constants are high ($k_a = 13.7 \times 10^9\text{ s}^{-1}$ at $20\text{ }^{\circ}\text{C}$) and the activation energies are low ($E_a = 2.2\text{ kcal mol}^{-1}$) compared with C–C molecules; however, their values for this small cycle are very similar to those for long linear chains of poly(methylphenylsiloxane). Thus, although the cycle is somewhat strained and has a greater fraction of isolated monomers and a smaller fraction of preformed dimers than the linear polymer, the main factor that determines excimer kinetics in both types of structures is their common conformational flexibility of the siloxane backbone. The kinetic mechanism developed succeeds in giving a fraction of photophysically hindered monomers (~ 0.23) in total agreement with the fraction of trans phenyl rings (0.23 determined from ^1H NMR) and also in giving a rate constant for excited monomer energy transfer independent of temperature.

Introduction

Siloxanes are well-known materials with application in many different fields. Their conformational and dynamic properties have been recently reviewed.¹ Cyclization² is an important characteristic of polysiloxanes that has been theoretically and experimentally measured by the cyclization equilibrium constant. Experimental results² agree with calculated values (with a modified Monte Carlo method)^{3,4} for intermediate and large cycles, but theoretical predictions fail for the smallest cycles as cyclic trisiloxanes. These shortest cycles require particular sequences of mutually interdependent rotational angles that have negligible probability in the rotational isomeric states (RIS) model employed in MC calculations. In fact, the RIS model has been questioned for polysiloxanes.^{5–7} With these conformational peculiarities it may be of special interest to determine dynamic magnitudes of cyclic trisiloxanes as (1,3,5-triphenyl-1,3,5-trimethyl-cyclotrisiloxane; CMPS3). This cyclic trimer is very much used as monomer to obtain the polymer by ring-opening polymerization. It has two isomers: cis and trans (Chart 1).²

CHART 1: Structures of the Isomers (Cis and Trans) of the Cyclic Trimer CMPS3, the Model Dimer DS, and the Model Monomer MS



Time-resolved fluorescence has been demonstrated to be useful in determining through direct measurements the rate constant of polymer segmental motions occurring in the nanosecond to picosecond time range.⁸ Such is the time range

[†] Instituto de Tecnologia Química e Biológica.

[‡] Instituto Superior Técnico.

[§] Universidad a Distancia.

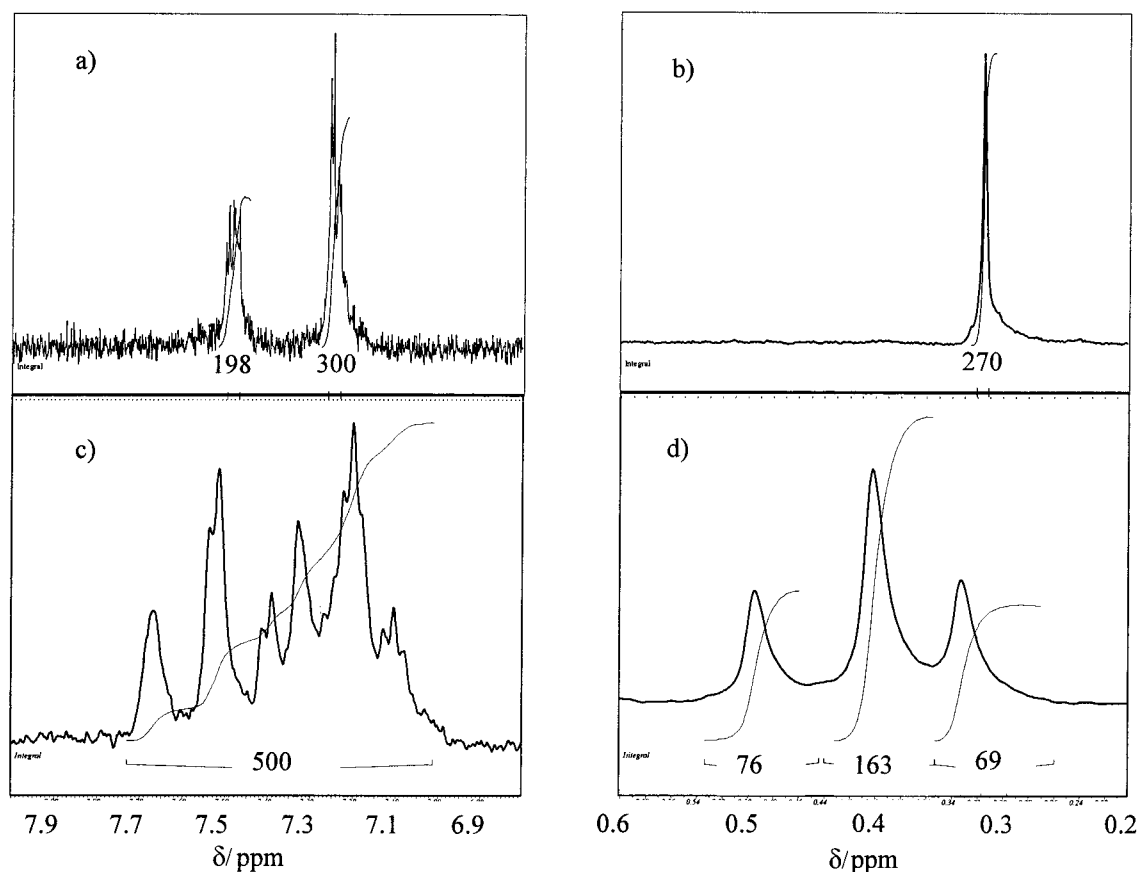


Figure 1. ^1H NMR spectra of DS phenyl groups (a), methyl groups (b), CMPS3 phenyl groups (c), and methyl groups (d) in deuterated methyl cyclohexane at 300 K. The numeric labels are relative integrals.

for segmental motions of polysiloxanes in dilute nonviscous solution. However, the fluorescence decays of linear polymer chains of poly(methylphenylsiloxane) (PMPS) are very complex (sums of at least three exponentials).⁸ The physical meaning of an intermediate time was attributed to the existence of monomers that stay isolated, that is, monomers that are unable to reach the excimer-forming conformation within the lifetime of the excited chromophore.^{8,9} The origin of such isolation of monomers in a linear chain is uncertain, but there are possible interpretations. One possible explanation is that groups of interacting chromophores in both sides of a phenyl group may "isolate it". This is plausible because excimer formation with such monomer implies either the separation of one of the interacting neighbors or the rotation of a more or less large portion of the chain as a whole. The separation of one of the interacting neighbors should be hindered because the interaction between adjacent phenyl groups in the siloxane chains is attractive, about -3 kcal mol^{-1} at the distance typical of the excimer-forming conformation.¹⁰

The consequences for the fluorescence decays of the presence of isolated monomers, which are hindered to form excimer, can be analyzed using the cycle CMPS3. In CMPS3, the bonding of the cycle puts one of the phenyls out of the possibility of reaching the excimer conformation with its neighbors. This happens with the "isolated" phenyl in the trans isomer. So the cycle is an ideal system to test the hypothesis of the third time coming from isolated monomers because in CMPS3 we know a priori (experimentally, as described in ^1H NMR Spectra section of Results) which fraction of monomers are unable to form excimers: ~ 0.23 .

The photophysics of CMPS3 has been previously studied by us but using steady-state fluorescence only.^{11,12}

Experimental Section

Phenylmethyldimethoxysilane (MS), 1,3-diphenyltetramethyldisiloxane (DS), and 1,3,5-triphenyl-1,3,5-trimethylcyclotrisiloxane (CMPS3) (Chart 1)¹³ were purchased from Petrarch and were purified by HPLC (Merck-Hitachi, Merck-RP18 column, solvent 70:30% THF/ H_2O , temperature 40°C , flow rate 0.7 mL/min). The commercial sample of CMPS3 was found to be in fact a mixture of several cyclic compounds (17% of CMPS3, retention time (rt) = 7.28 min; 24.6% of CMPS4, rt = 8.55 min; 25% of CMPS5, rt = 9.55 min; 17.7% of CMPS6, rt = 10.67 min),¹⁴ as identified by mass spectrometry (Kratos MS 25 RE). Methylcyclohexane (MCH) from BDH (laboratory reagent) was purified as previously described.¹⁵

Solutions of absorbance less than 0.5 at the excitation wavelength (260 nm) were degassed by the freeze-pump-thaw technique (six cycles at 10^{-4} Torr) and sealed. Solutions of the monomeric model (MS) were prepared with exactly the same absorbance at the excitation wavelength (the monomeric model is a monochromophoric compound that enjoys photophysical properties identical to those of the monomer but cannot form excimers).¹³

Steady-state fluorescence measurements were performed with a Spex Fluorolog F212I.

The fluorescence decays of the same solutions employed in steady-state measurements, were measured, as a function of temperature, by the time-correlated single photon counting technique (SPC), as described before.^{15,16} An Ar^+ -pumped frequency-tripled Ti:sapphire picosecond laser system (Spectra Physics Inc.) was the excitation source ($\lambda_{\text{ex}} = 260 \text{ nm}$, repetition rate 827 kHz). Alternate collection of pulse and sample was performed (10^3 counts at the maximum per cycle) until 10^4

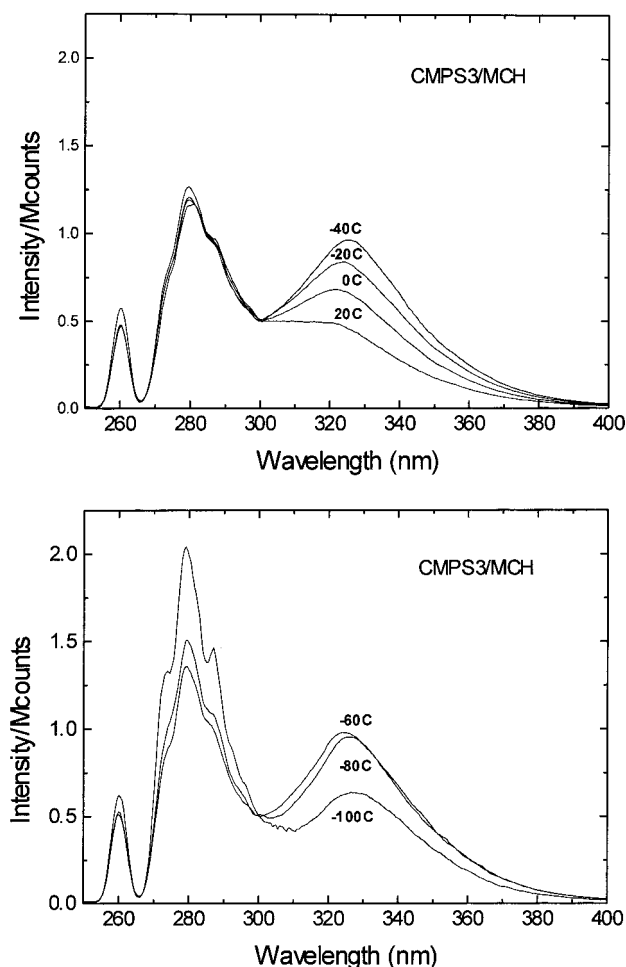


Figure 2. Fluorescence spectra of CMPS3 (MCH solution) at several temperatures.

counts at the maximum were acquired. The fluorescence decays were deconvoluted in a Micro Vax 3100, using an updated version of George Striker's program,¹⁷ which allows for single and global analysis and automatic shift correction.

¹H NMR spectra of CMPS3 (5.1×10^{-4} M), DS (7.7×10^{-4} M), and MS (1.5×10^{-3} M), in deuterated methylcyclohexane (99.5% deuteration, Cambridge Isotope Laboratories Inc.), at 300 K were obtained with a Bruker AMX-300 spectrometer. The solvent peaks were used to calibrate the chemical shifts.

Results

¹H NMR Spectra. The ¹H NMR spectra of MS and DS are similar, both presenting one singlet for the methyl protons (around 0.3 ppm) and two singlets for the phenyl protons (around 7.3 and 7.5 ppm). Also, three signals appear for CMPS3 (Figure 1), but now they are triplets: (0.335, 0.402, 0.497); (7.10, 7.20, 7.33); (7.39, 7.51, 7.67) (ppm). The integrals of these three triplets are proportional to 3, 3, 2, respectively (3 methyl, 3 + 2 phenyl). The triplet form can be attributed to the existence of three different neighborhoods for the methyl (Me) phenyl (Ph) protons in CMPS3 (Me-Me; Me-Ph = Ph-Me; Ph-Ph). The best resolved triplet is that of the methyl group. The peak at 0.497 ppm is assigned to the cis isomer (Chart 1c) and the remaining two peaks to the trans isomer: 0.335 ppm to the methyl group that is trans with respect to the other two groups, and 0.402 ppm to these other groups (Chart 1d).

CMPS3 has a total of eight different configurations possible, two of which are cis and six of which are trans. The relative

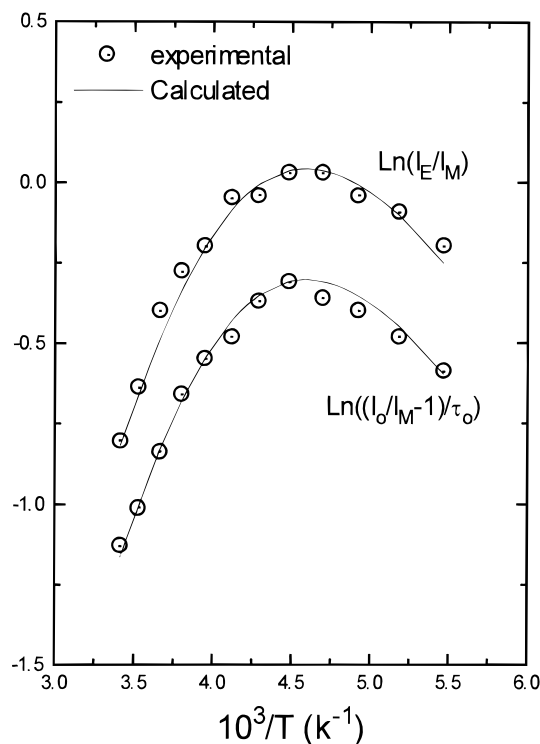


Figure 3. Plot of $\ln\{(I_0/(I_M - 1))/\tau_0\}$ and $\ln(I_E/I_M)$ as functions of reciprocal temperature. The circles are experimental points from steady-state measurements, and the line is the curve calculated with the kinetic parameters (see text).

areas of the peaks in the methyl triplet, 23% (0.335 ppm), 52% (0.402 ppm), and 25% (0.497 ppm), are in agreement with the expected populations when total randomness or equal probability of configurations (25, 50, 25%) is assumed.

Steady-State Fluorescence. The fluorescence spectra of CMPS3 were measured in MCH at several temperatures in the range 20 to -100 °C. Within this temperature range, two bands, typical of monomer (280 nm) and excimer (330 nm) emissions, can be seen (Figure 2). The monomer fluorescence intensity increases from 20 to -100 °C, while that of the excimer increases from 20 to -60 °C and then decreases with further decreasing temperature. The overall temperature dependence is shown in Figure 3, in the form of Stevens–Ban plots. Here, I_M is the monomer peak intensity, I_E is the excimer band intensity, I_0 is the emission intensity of the monomeric model compound MS, and τ_0 is its fluorescence lifetime.¹³ I_M and I_0 are measured at 275 nm, I_E is measured at 330 nm on the spectra of CMPS3, after subtracting the spectra of MS obtained under the same conditions and normalized at 280 nm.

The plot in Figure 3 shows the expected bell-shaped dependence, with positive slope, corresponding to the HTL region, a maximum, and then a change to negative slope, typical of the LTL. The intersection of the LTL and HTL linear extrapolations defines the temperature for the crossover between both regimes as -30 °C (somewhat below the previous estimate of -20 °C).¹²

The activation energy of excimer formation (E_a) could be calculated from the LTL slope in Figure 3 type plots, provided that the Birks scheme would apply. We will see that this is not the case for CMPS3.

Time-Resolved Fluorescence. Both monomer and excimer fluorescence decays of CMPS3 in MCH can only be fitted with sums of three exponentials (Figure 4). Global analysis of these decays (imposing common decay times for monomer and

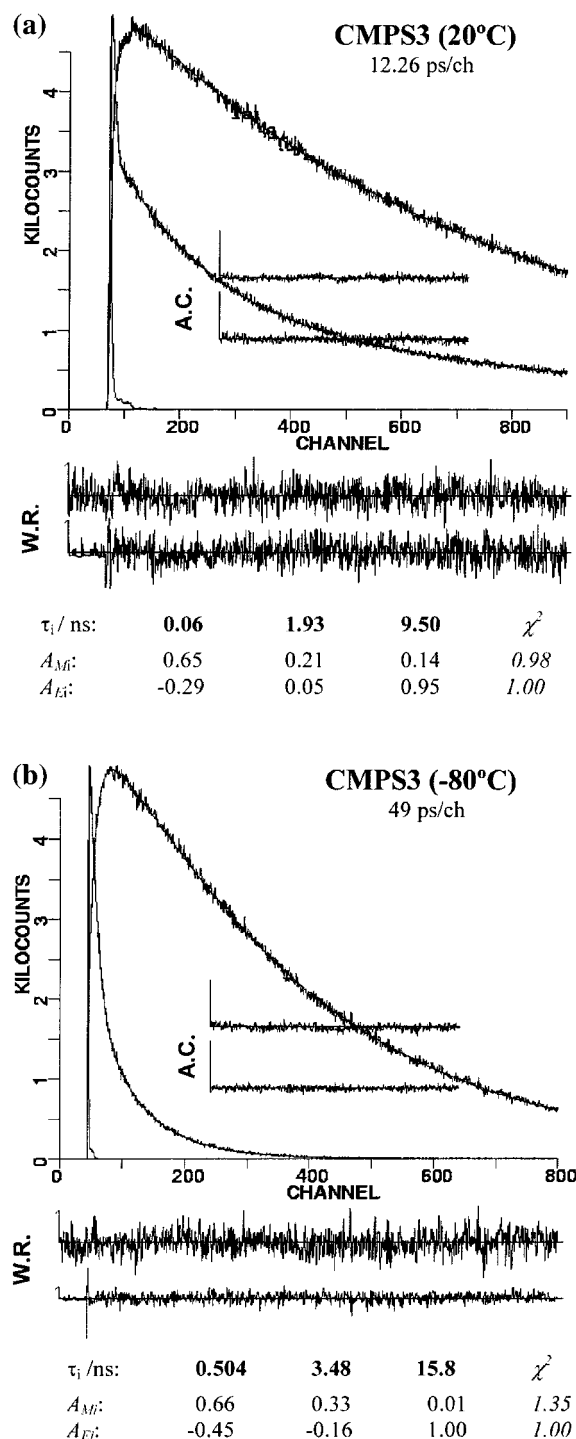


Figure 4. Fluorescence decays of CMPS3 (monomer and excimer) in MCH at (a) 20 °C and (b) -80 °C and results from global analysis with decay times (τ_i), amplitudes (A_{Mi} , A_{Ei}), and fitting parameters (autocorrelation function, A.C.; weighted residuals, W.R.; and χ^2 values) listed.

excimer) still gives excellent fits when three exponentials are used. Examples of such decays at two temperatures (20 and -80 °C) are shown in Figure 4. (τ are the common decay times, A_M and A_E the respective monomer and excimer amplitudes, and χ^2 the chi-squared value of the fit). The three times can be appreciated visually in the monomer curve, where there is first a very fast decay, followed by a slower one, and finally a long, slow tail. The short time is in the picosecond range (61–504 ps from 20 to -80 °C), while the intermediate and the long

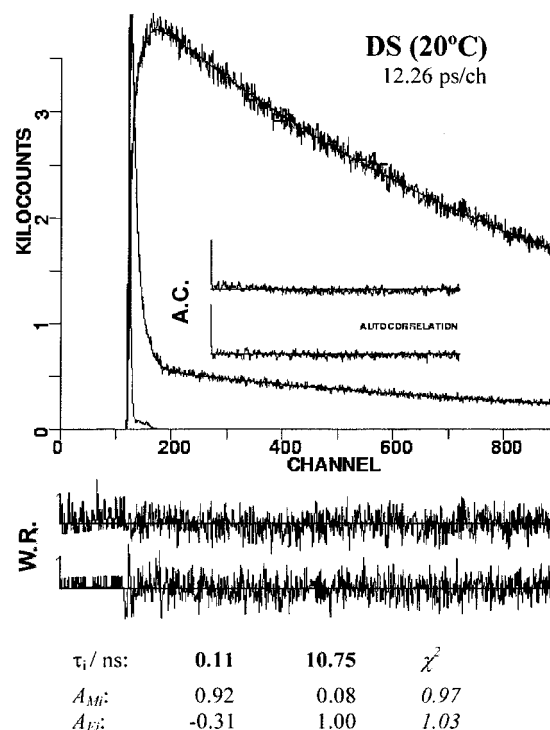


Figure 5. Fluorescence decays of DS (monomer and excimer) in MCH at 20 °C and results from global analysis (as in Figure 4).

times are in the nanosecond range (respectively, 1.93–3.48 and 9.5–15.8 ns, from 20 to -80 °C).

This pattern can be compared to that of the dimer DS, whose decays (also at 20 °C) are shown in Figure 5. In the dimer, only two times are detected and triexponential functions do not improve the statistical standard functions of the fit: distribution of the residuals, autocorrelation function of the residuals, and χ^2 value. The two DS fluorescence decay times are similar to the short one and the long one of CMPS3, the intermediate time being nonexistent here.

Discussion

Triple exponential decays usually mean three kinetically coupled species. In this case, one monomer, one excimer, and a third species. Figure 6 shows the temperature dependence of the three reciprocal decay times and respective amplitudes in the monomer and excimer decays of CMPS3 in MCH. First, note that the temperature dependence of the short, λ_3 , and long, λ_1 , reciprocal decay times and their amplitudes are typical of Birks' monomer–excimer kinetics: λ_3 and λ_1 decrease with lowering temperature, and at the lowest temperatures, the slow process with the long time has almost disappeared in the monomer (i.e., $A_{M1} \approx 0$) because at this low temperature, the excimer back-dissociation to monomer is frozen.

Also, note that the contribution of the intermediate time in the monomer decays (A_{M2}) is large at all temperatures and increases with lowering temperature. Thus, its origin is clearly a monomeric species, and that can only be the “isolated” phenyl in the trans isomer. The temperature dependence of the intermediate reciprocal decay time, λ_2 , is qualitatively similar to that of τ_0^{-1} , but there is no quantitative coincidence; λ_2 is larger than τ_0^{-1} in the whole range of temperatures studied here, and thus, that component may not be ascribed to strictly isolated chromophores unable to interact with the others, as in copolymers with very low content of methylphenylsiloxane.¹⁸ The isolated excited monomers must participate in the kinetics of

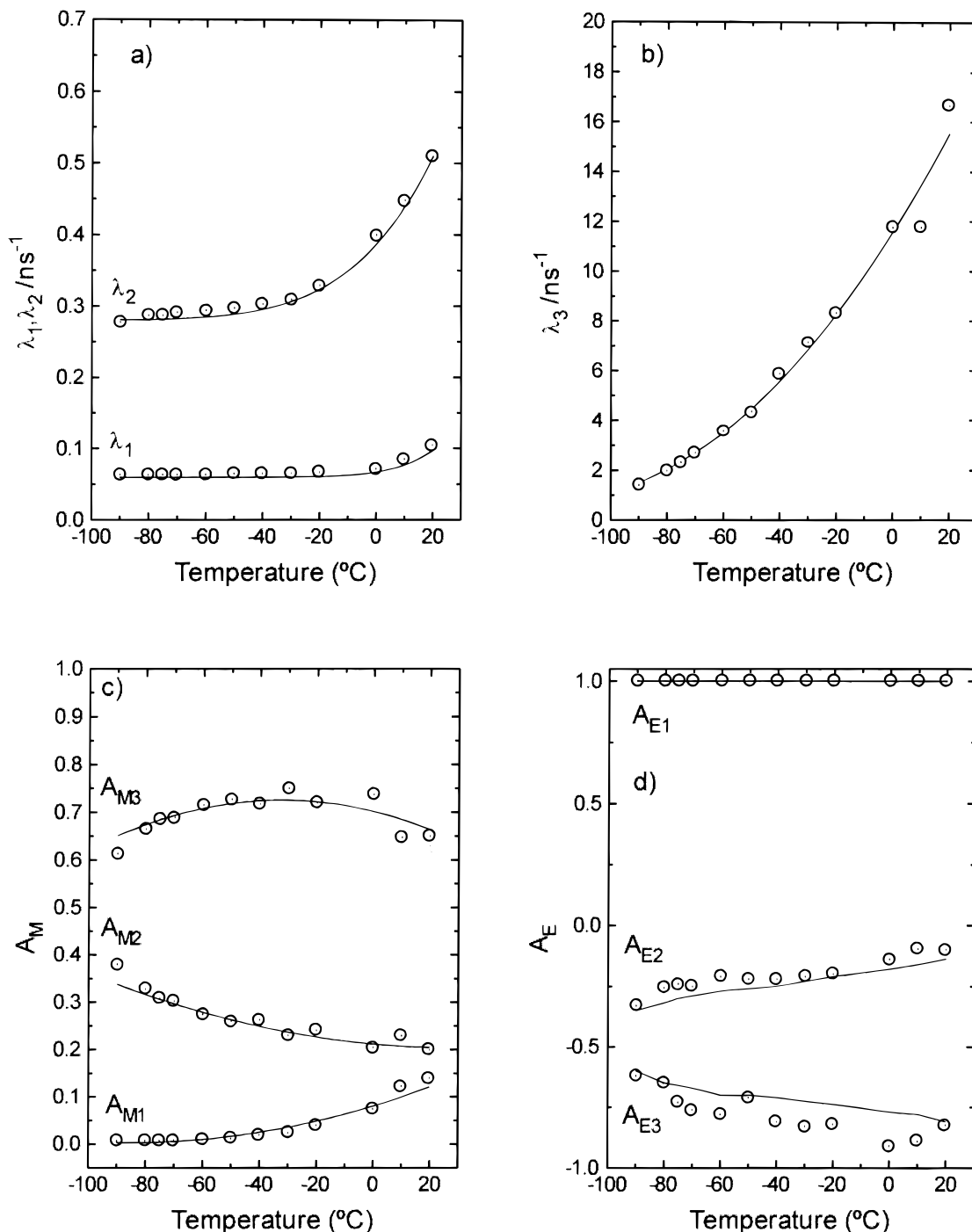


Figure 6. Global fit parameters of the fluorescence decays of CMPS3 in MCH as a function of temperature: (a, b) reciprocal decay times λ_i , (c) monomer amplitudes A_{Mi} , and (d) excimer amplitudes A_{Ei} . The lines are theoretical curves calculated with the parameters obtained from the kinetic model.

excimer formation, and that can only be via energy transfer to the excimer-forming monomers.

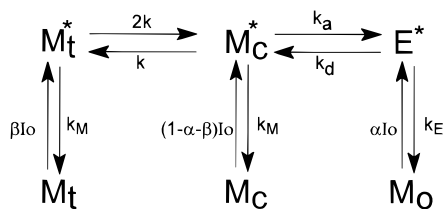
In Figure 6d, we can also see that the sum of the two negative amplitudes of the excimer decay does not compensate the positive one, A_{E1} . This is mostly due to residual emission of monomer at the wavelength at which the excimer has been measured ($\lambda_{\text{em}} = 330 \text{ nm}$). There, even a few percent of monomer contribution strongly affects the value of A_{E3} because of the fact that τ_3 is very short (and A_{M3} is large) with respect to the other times. A correction of the excimer amplitudes, using fluorescence spectra, leads to sums of excimer amplitudes close to zero within the errors of the correction procedure.

On the other hand, the sums of the noncorrected amplitudes at wavelengths longer than 330 nm become slightly less positive but never approach zero, which may indicate¹⁹ the existence of ground-state preformed dimers that give excimers by direct absorption of light as was previously advanced for CMPS3 from steady-state results.¹²

Therefore, we proceed to develop the kinetic scheme needed with proper consideration of isolated monomers and preformed dimers.

Mechanism and Kinetic Equations. The mechanism here considered (Scheme 1) includes three kinetically coupled species (two monomers and one excimer). These are (1) the isolated

SCHEME 1: Kinetic Mechanism



phenyl group in the trans isomer (M_t^*), which can decay to the ground state (k_M) or transfer the excitation to any of the other two phenyl groups ($2k$), (2) the remaining phenyl groups (M_c^*), which can form excimers (k_a), back-transfer energy (k), or decay to the ground state (k_M), (3) the excimer (E^*), which can dissociate back to the excited monomer M_c^* (k_d) or decay to ground-state monomers (k_E). The model also takes into account the possibility that excimers can be formed not only by the usual dynamic mechanism with rate constant k_a but also by direct absorption of light of α ground-state monomer units forming ground-state dimers (M_0). The molar fraction of isolated ground-state monomers (M_t) is represented by β , and I_0 is the rate of light absorption by all monomers at the excitation wavelength.

The time evolution of the concentration vector of the three species in Scheme 1 is ruled by the following differential equation:

$$\frac{d}{dt} \begin{bmatrix} M_t^* \\ M_c^* \\ E^* \end{bmatrix} = \begin{bmatrix} -(2k + k_M) & k & 0 \\ 2k & -(k + k_M + k_a) & k_d \\ 0 & k_a & -(k_E + k_d) \end{bmatrix} \times \begin{bmatrix} M_t^* \\ M_c^* \\ E^* \end{bmatrix} \quad (1)$$

where M_t^* , M_c^* , and E^* are the excited-state concentrations of the species.

Integration of eq 1 leads to

$$\begin{bmatrix} M_t^* \\ M_c^* \\ E^* \end{bmatrix} = \begin{bmatrix} a_{11} & a_{12} & a_{13} \\ a_{21} & a_{22} & a_{23} \\ a_{31} & a_{32} & a_{33} \end{bmatrix} \times \begin{bmatrix} e^{-\lambda_1 t} \\ e^{-\lambda_2 t} \\ e^{-\lambda_3 t} \end{bmatrix} \quad (2)$$

where $\lambda_1, \lambda_2, \lambda_3$ are the *eigenvalues* of the transformation matrix and the a_{ij} ($i, j = 1, 2, 3$) are the linear combinations of the *eigenvectors* basis set obeying the initial conditions

$$\sum_{j=1}^3 a_{1j} = \beta \quad (3)$$

$$\sum_{j=1}^3 a_{2j} = 1 - \alpha - \beta \quad (4)$$

$$\sum_{j=1}^3 a_{3j} = \alpha \quad (5)$$

The *eigenvalues* λ_j are the roots of the characteristic equation of the transformation matrix

$$\lambda^3 - \lambda^2(2X + k + k_a + Y) + \lambda[Y(X + k_a) + (X + k)(Y + X + k_a) - k_a k_d - 2k^2] + (X + k)k_a k_d + 2k^2 Y - Y(X + k_a)(X + k) = 0 \quad (6)$$

where $X = k_a + k_M$ and $Y = k_E + k_d$.

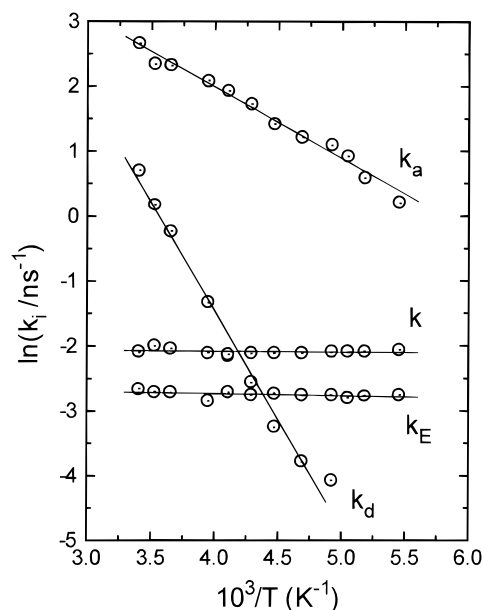


Figure 7. Rate constants (defined in Scheme 1) as a function of temperature.

The preexponential coefficients (a_{ij}) are also functions of k , k_a , k_d , k_E , k_M , α , and β . These functions are given in the Appendix (eqs A.1–A.9).

Data Analysis. At the monomer emission wavelength, the experimental fluorescence intensity is the sum of emissions of nonisolated (M_c) and isolated monomers (M_t), and its time dependence is given by

$$I_M(t) = I_{M_c}(t) + I_{M_t}(t) = \sum_{j=1}^3 A_{Mj} \exp(-\lambda_j t) \quad (7)$$

The excimer emission is also given by a sum of three exponentials:

$$I_E(t) = \sum_{j=1}^3 A_{Ej} \exp(-\lambda_j t) \quad (8)$$

The experimental amplitudes A_{Mj} and A_{Ej} are related to the coefficients of linear transformation of the *eigenvectors* by

$$A_{Mj} = k_{fM} f_M (a_{1j} + a_{2j}) \quad (j = 1, 2, 3) \quad (9)$$

$$A_{Ej} = k_{fE} f_E a_{3j} \quad (j = 1, 2, 3) \quad (10)$$

where k_{fM} and k_{fE} are the monomer and excimer radiative rate constants and f_M and f_E are instrument factors.

The evaluation of the seven unknowns in Scheme 1 (k , k_a , k_d , k_E , k_M , α , and β) requires at least six independent equations (k_M is measured with the monomeric model compound) and six experimental parameters (besides k_M). The number of available experimental parameters are seven: λ_1 , λ_2 , λ_3 , A_{M3}/A_{M2} , A_{M3}/A_{M1} , A_{E3}/A_{E2} , and A_{E3}/A_{E1} .

The numerical evaluation of the unknowns was done using the “fmins” routine (AT-MATLAB package) to minimize the residuals of the seven following relations at each temperature:

$$\sum_{i=1}^3 \lambda_i - (2X + k + k_a + Y) = 0 \quad (11)$$

$$\sum_{\substack{i,j=1 \\ j>i}}^3 \lambda_i \lambda_j - (Y(X + k_a) + (X + k)(Y + X + k_a) - k_a k_d - 2k^2) = 0 \quad (12)$$

$$\lambda_1 \lambda_2 \lambda_3 - (Y(X + k_a)(X + k) - (X + k)k_a k_d - 2k^2 Y) = 0 \quad (13)$$

$$\frac{A_{M3}}{A_{M2}} - \left(\frac{a_{13} + a_{23}}{a_{12} + a_{22}} \right) = 0 \quad (14)$$

$$\frac{A_{M3}}{A_{M1}} - \left(\frac{a_{13} + a_{23}}{a_{11} + a_{21}} \right) = 0 \quad (15)$$

$$\frac{A_{E3}}{A_{E2}} - \left(\frac{a_{33}}{a_{32}} \right) = 0 \quad (16)$$

$$\frac{A_{E3}}{A_{E1}} - \left(\frac{a_{33}}{a_{31}} \right) = 0 \quad (17)$$

The output results are shown in Figures 7 and 8 and Table 1.

Rate Constants k_a , k_d , k_M , k_E . k_a values are large (Table 1), denoting that excimer formation is a fast process, and its temperature variation is relatively weak (see E_a in Table 1). These results are very similar to those found in linear polymers of PMPS, where the k_a and E_a values are of this same order for any chain length (13–16 ns⁻¹ at 20 °C and 2.3–2.9 kcal mol⁻¹).⁸ Thus, the restriction imposed by ring closure little affects the mobility related to excimer formation. This strongly supports the idea that only chromophore reorientation is needed both in linear PMPS and CMPS3 to form excimers.

The CMPS3 k_d values (Table 1) are much lower than those of k_a and its temperature variation more pronounced, as corresponds to the existence of a binding energy ($-\Delta H \approx 4.4$ kcal mol⁻¹) opposing excimer dissociation.

The rate for excimer decay, k_E , does not change with temperature in all the ranges studied, contrary to what happens with the rate for monomer decay, $k_M = \tau_0^{-1}$, which is strongly temperature-dependent. This is so because in the case of k_M the dominant term, at temperatures above -50 °C, is the nonradiative decay, whereas the radiative decay is the predominant process in the case of excimer decay, in the whole range of temperature.

Let us come now to the parameters directly related to the assumptions about isolated monomers and preformed dimers, namely, the fractions α and β and the rate constant k .

Rate Constant of Energy Transfer, k . The k values are from 1 to 2 orders of magnitude lower than k_a and temperature-independent, as expected for an energy-transfer process. Besides, $2k$ values (0.25 ns⁻¹) are about the same for PMPS⁸ and CMPS3 (0.3 ns⁻¹), as expected for the same chromophores in the same local environment with two neighboring phenyl groups in preformed dimers. Both values are also close to the rate constant of energy transfer, which is calculated from the Förster critical distance ($R_0 = 7.25$ Å for dimethoxymethylphenylsilane)⁸ and the average distance between phenyl groups in the trans isomer ($R = 7.08$ Å): $k = k_M(R_0/R)^6 = 0.31$ ns⁻¹.

Molar Fractions of Isolated Monomers and Preformed Dimers. The fraction β of monomers that are isolated should also come out independent of temperature. In Figure 8 we see that β actually is temperature-independent. Not only that, but the values of this fraction scatter little (0.21–0.26) and their mean value is very close to the experimental value of ~ 0.23 ,

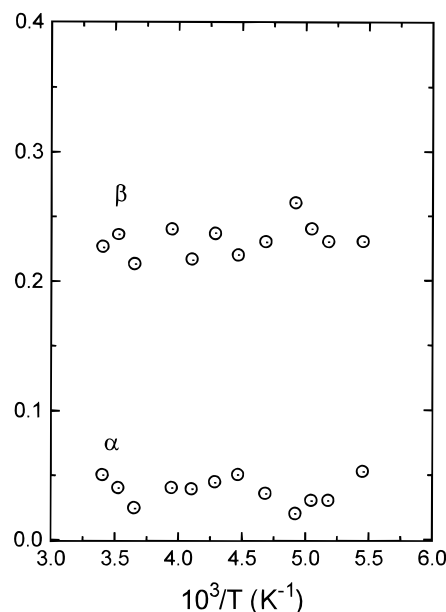


Figure 8. Fraction of isolated monomers and preformed dimers (defined in Scheme 1) as a function of temperature.

TABLE 1: Summary of Rate Constants, Activation Energies, and Excimer Binding Enthalpy Obtained for CMPS3 in MCH Solution from Time-Resolved Results

$k_a^{20^\circ\text{C}}/10^9 \text{ s}^{-1}$	13.7 ± 0.5
$k_d^{20^\circ\text{C}}/10^9 \text{ s}^{-1}$	1.64 ± 0.4
$k/10^9 \text{ s}^{-1}$	0.13 ± 0.01
$k_a^0/10^{12} \text{ s}^{-1}$	0.62 ± 0.13
$k_d^0/10^{15} \text{ s}^{-1}$	0.14 ± 0.1
$E_a/\text{kcal mol}^{-1}$	2.2 ± 0.1
$E_d/\text{kcal mol}^{-1}$	6.6 ± 0.3
$\Delta H/\text{kcal mol}^{-1}$	4.4 ± 0.4
α	0.04 ± 0.015
β	0.23 ± 0.02

which corresponds to the fraction of chromophores configurationally isolated.

The values of α are so small at any temperature (Figure 8) that the existence of preformed dimers is questionable.

Parameters from Steady-State Data. When steady-state conditions are applied to eq 1, the following relations of the fluorescence intensities of the monomer (I_M), excimer (I_E), and the model compound (I_0) are derived:

$$\frac{I_E}{I_M} = \frac{k_{IE}}{k_{IM}} \frac{\alpha k_M(3k + k_M) + k_a(2k + (1 - \beta)k_M)}{(k_d + (1 - \alpha)k_E)(3k + k_M) + \beta k_E k_a} \quad (18)$$

$$\left(\frac{I_0}{I_M} - 1 \right) k_M = \frac{\alpha k_M(3k + k_M) + k_a(2k + (1 - \beta)k_M)}{(k_d + (1 - \alpha)k_E)(3k + k_M) + \beta k_E k_a} k_E \quad (19)$$

These equations reduce to the well-known Stevens–Ban equations,

$$\frac{I_E}{I_M} = \frac{k_{IE}}{k_{IM}} \frac{k_a}{k_d + k_E} \quad (20)$$

$$\left(\frac{I_0}{I_M} - 1 \right) k_M = \frac{k_a}{k_d + k_E} k_E \quad (21)$$

when $\alpha = \beta = k = 0$ (Birks scheme).

Inspection of eqs 18 and 19 shows that the slopes in the LTL or HTL regions are not equal to $-E_a/R$ and $-\Delta H/R$ and have

no physical meaning. Furthermore, apparent k_a values, estimated from the LTL region, are in fact the values of a complex function of all the kinetic parameters and also have no physical meaning. In fact, these values are^{11,12} much lower than the correct k_a values from time-resolved data. This discrepancy is now clearly understood in light of the kinetic mechanism developed here.

Acknowledgment. Financial support from ITQB and Acções Integradas Luso-Espanholas E-51/97 (Portugal) and DGICYT (Spain, Grant PB95-0247) is gratefully acknowledged. Fernando B. Dias acknowledges FCT (Portugal) for the Grant PRAXIS XXI/9017/96 and João C. Lima thanks ITQB for a postdoctoral grant. We give thanks to George Striker for making his deconvolution program available to us.

Appendix

$$a_{11} = Ma_{21} \quad (\text{A.1})$$

$$a_{12} = La_{22} \quad (\text{A.2})$$

$$a_{13} = Ja_{23} \quad (\text{A.3})$$

$$a_{21} = (1 - \alpha - \beta) - a_{22} - a_{23} \quad (\text{A.4})$$

$$a_{22} = \frac{DC - AF}{DB - EA} \quad (\text{A.5})$$

$$a_{23} = \frac{BF - EC}{DB - EA} \quad (\text{A.6})$$

$$a_{31} = Ia_{21} \quad (\text{A.7})$$

$$a_{32} = Ha_{22} \quad (\text{A.8})$$

$$a_{33} = Ga_{23} \quad (\text{A.9})$$

where the parameters A , B , ..., and M are given by the following relations:

$$A = \frac{k_a}{Y - \lambda_3} - \frac{k_a}{Y - \lambda_1} \quad (\text{A.10})$$

$$B = \frac{k_a}{Y - \lambda_2} - \frac{k_a}{Y - \lambda_1} \quad (\text{A.11})$$

$$C = \alpha - (1 - \alpha - \beta) \frac{k_a}{Y - \lambda_1} \quad (\text{A.12})$$

$$D = \frac{k}{(X + k) - \lambda_3} - \frac{k}{(X + k) - \lambda_1} \quad (\text{A.13})$$

$$E = \frac{k}{(X + k) - \lambda_2} - \frac{k}{(X + k) - \lambda_1} \quad (\text{A.14})$$

$$F = \beta - (1 - \alpha - \beta) \frac{k}{(X + k) - \lambda_1} \quad (\text{A.15})$$

$$G = \frac{k_a}{Y - \lambda_3} \quad (\text{A.16})$$

$$H = \frac{k_a}{Y - \lambda_2} \quad (\text{A.17})$$

$$I = \frac{k_a}{Y - \lambda_1} \quad (\text{A.18})$$

$$J = \frac{k}{(X + k) - \lambda_3} \quad (\text{A.19})$$

$$L = \frac{k}{(X + k) - \lambda_2} \quad (\text{A.20})$$

$$M = \frac{k}{(X + k) - \lambda_1} \quad (\text{A.21})$$

References and Notes

- (1) Horta, A.; Piérola, I. F.; Maçanita, A. L. In *The Polymeric Materials Encyclopedia. Synthesis, Properties and Applications*; Salamone, J. C., Ed.; CRC Press: Boca Raton, FL, 1996; Vol. 8, pp 6391–6402.
- (2) Semlyen, J. A., Ed. *Cyclic Polymers*; Elsevier: London, 1986.
- (3) Rubio, A.; Freire, J. J.; Horta, A.; Piérola, I. F. *Macromolecules* **1991**, *24*, 5167.
- (4) Rubio, A.; Freire, J. J.; Horta, A.; Piérola, I. F. *Macromolecules* **1991**, *24*, 3121.
- (5) Horta, A.; Maçanita, A. L.; Freire, J. J.; Piérola, I. F. *Polym. Int.* **1999**, *48*, 665.
- (6) Horta, A.; Piérola, I. F.; Maçanita, A. L. *Macromolecules*, submitted.
- (7) Bahar, I.; Zúñiga, I.; Dodge, R.; Mattice, W. L. *Macromolecules* **1991**, *24*, 2986.
- (8) Lima, J. C.; Maçanita, A. L.; Dias, F. B.; Horta, A.; Piérola, I. F. Manuscript in preparation.
- (9) Maçanita, A. L. (in collaboration with Lima, J. C.; Dias, F. B.; Campos, P.; Horta, A.; Piérola, I. F.) In *Plenary Lectures of the III Congreso de Fotoquímica*; Armesto, D., Orellana, G., Piérola, I. F., Eds.; UNED: Madrid, 1996.
- (10) Freire, J. J.; Piérola, I. F.; Horta, H. *Macromolecules* **1996**, *29*, 5143.
- (11) Salom, C.; Semlyen, J. A.; Clarson, S.; Hernández-Fuentes, I.; Maçanita, A.; Horta, A.; Piérola, I. F. *Macromolecules* **1991**, *24*, 6827.
- (12) Maçanita, A. L.; Horta, A.; Piérola, I. F. *Macromol. Symp.* **1994**, *84*, 365.
- (13) Maçanita, A. L.; Danesh, P.; Peral, F.; Horta, A.; Piérola, I. F. *J. Phys. Chem.* **1994**, *98*, 6548.
- (14) CMPSx means cycle of x monomer units.
- (15) Maçanita, A. L.; Piérola, I. F.; Horta, A. *Macromolecules* **1991**, *24*, 1293.
- (16) Maçanita, A. L.; Costa, F. P.; Costa, S. M. B.; Melo, E. C.; Santos, H. *J. Phys. Chem.* **1989**, *93*, 336.
- (17) Striker, G. In *Deconvolution and Reconvolution of Analytical Signals*; Bouchy, M., Ed.; DPIC: Nancy, France 1982.
- (18) Maçanita, A. L.; Horta, A.; Piérola, I. F. *Macromolecules* **1994**, *27*, 3797.
- (19) Maçanita, A. L.; Horta, A.; Piérola, I. F. *Macromolecules* **1994**, *27*, 958.